

# Interferon priming enables cells to partially overturn the SARS coronavirus-induced block in innate immune activation

Thomas Kuri,<sup>1</sup> Xiaonan Zhang,<sup>2</sup> Matthias Habjan,<sup>1</sup>  
Luis Martínez-Sobrido,<sup>3</sup> Adolfo García-Sastre,<sup>4</sup> Zhenghong Yuan<sup>2</sup>  
and Friedemann Weber<sup>1</sup>

Correspondence  
Friedemann Weber  
friedemann.weber@  
uniklinik-freiburg.de

<sup>1</sup>Abteilung Virologie, Institut für Medizinische Mikrobiologie und Hygiene, Universität Freiburg, D-79008 Freiburg, Germany

<sup>2</sup>Research Unit, Shanghai Public Health Clinical Center, and Key Laboratory of Medical Molecular Virology, Fudan University, Shanghai, PR China

<sup>3</sup>School of Medicine and Dentistry, University of Rochester, Rochester, NY 14642, USA

<sup>4</sup>Department of Microbiology, Department of Medicine (Division of Infectious Diseases) and Global Health and Emerging Pathogens Institute, Mount Sinai School of Medicine, New York, NY 10029, USA

SARS coronavirus (SARS-CoV) is known to efficiently suppress the induction of antiviral type I interferons (IFN- $\alpha/\beta$ ) in non-lymphatic cells through inhibition of the transcription factor IRF-3. Plasmacytoid dendritic cells, in contrast, respond to infection with production of high levels of IFNs. Here, we show that pretreatment of non-lymphatic cells with small amounts of IFN- $\alpha$  (IFN priming) partially overturns the block in IFN induction imposed by SARS-CoV. IFN priming combined with SARS-CoV infection substantially induced genes for IFN induction, IFN signalling, antiviral effector proteins, ubiquitination and ISGylation, antigen presentation and other cytokines and chemokines, whereas each individual treatment had no major effect. Curiously, however, despite this typical IFN response, neither IRF-3 nor IRF-7 was transported to the nucleus as a sign of activation. Taken together, our results suggest that (i) IFN, as it is produced by plasmacytoid dendritic cells, could enable tissue cells to launch a host response to SARS-CoV, (ii) IRF-3 and IRF-7 may be active at subdetectable levels, and (iii) SARS-CoV does not activate IRF-7.

Received 22 May 2009  
Accepted 18 July 2009

## INTRODUCTION

SARS coronavirus (SARS-CoV) is the causative agent of severe acute respiratory syndrome (SARS), a life-threatening human disease that has recently emerged in China (Drosten *et al.*, 2003; Ksiazek *et al.*, 2003; Kuiken *et al.*, 2003; Peiris *et al.*, 2003b). SARS-CoV causes high fever, myalgia, dry cough and lymphopenia, and around 30% of patients develop an atypical pneumonia (Denison, 2004; Peiris *et al.*, 2004). The worldwide epidemic in spring 2003 resulted in over 8000 cases with 774 deaths (WHO, 2004).

SARS-CoV is known to be sensitive to the antiviral action of type I interferons (IFN- $\alpha/\beta$ ) both in cell culture and *in vivo* (Cinatl *et al.*, 2003; Haagmans *et al.*, 2004; Stroher *et al.*, 2004).

IFNs are synthesized and secreted by infected cells and stimulate expression of potent antiviral proteins (Sadler & Williams, 2008; Samuel, 2001). IFN induction in tissue cells occurs mainly by an intracellular pathway. Hallmark molecules of virus infection, such as double-stranded RNA (dsRNA) or 5'-triphosphorylated single-stranded RNA, are recognized by cellular receptors such as RIG-I and MDA5, and activate a signalling chain resulting in phosphorylation of the transcription factor IRF-3 (Pichlmair & Reis e Sousa, 2007; Yoneyama & Fujita, 2008). IRF-3 is a member of the IFN-regulatory factor (IRF) family and plays a central role in the transactivation of the IFN- $\beta$  promoter (Hiscott, 2007). Phosphorylated IRF-3 homodimerizes and moves into the nucleus, where it initiates IFN- $\beta$  mRNA synthesis (Suhara *et al.*, 2002; Weaver *et al.*, 1998). This first-wave IFN triggers expression of a related factor, IRF-7, which is present only in low amounts in unstimulated fibroblasts (Honda *et al.*, 2005). IRF-7 can be activated by the same pathway as IRF-3

Two supplementary tables showing oligonucleotide primers used for RT-PCR analyses and global gene expression in IFN-primed and SARS-CoV-infected 293Ip cells are available with the online version of this paper.

(Caillaud *et al.*, 2005), leading to a positive-feedback loop that initiates the synthesis of several IFN- $\alpha$  subtypes as the second-wave IFNs (Marie *et al.*, 1998).

Despite its sensitivity against IFN- $\alpha/\beta$ , SARS-CoV grows at a fast rate and spreads rapidly to different organs, including the lungs (Gu *et al.*, 2005; Peiris *et al.*, 2003a). We have shown previously that, in non-lymphatic cells infected with SARS-CoV, neither dimerization nor stable nuclear accumulation of IRF-3 occurs (Spiegel *et al.*, 2005). Consequently, infected cells do not transcribe the IFN- $\beta$  gene (Spiegel *et al.*, 2005), although the IFN inducer dsRNA is generated by the virus (Weber *et al.*, 2006). In contrast, plasmacytoid dendritic cells (pDCs), which are the major IFN producers of the immune system, are able to release significant amounts of IFN after SARS-CoV infection (Cervantes-Barragan *et al.*, 2007).

It is known that pretreatment of cells with small amounts of IFN ('priming') can enhance the response to viral infection significantly (Erlandsson *et al.*, 1998; Phipps-Yonas *et al.*, 2008; Stewart *et al.*, 1971). We therefore wondered whether IFN, as it is produced by infected pDCs, could alter the response of tissue cells to SARS-CoV infection. Our study indicates that IFN priming indeed enables cells to overturn the virus-imposed block in IFN induction in such a way that infected cells start to produce low but detectable amounts of IFNs, resulting in a typical IFN response. Nonetheless, no detectable signs of IRF-3 or IRF-7 activation were observed, indicating that the various anti-IFN mechanisms employed by the virus are still functioning to some extent.

## METHODS

**Cells, viruses, cytokines and plasmids.** Simian Vero cells, human A549 cells and human 293 low-passage (1p) cells were cultivated in Dulbecco's modified Eagle's medium supplemented with 10% fetal calf serum. The 293p cell clone (Graham *et al.*, 1977) was purchased from Microbix Biosystems and cells were used between passages 38 and 48. The FFM-1 isolate of SARS-CoV was kindly provided by Stephan Becker, University of Marburg, Germany. Rift Valley fever virus strain Clone 13 was kindly provided by Michèle Bouloy, Institut Pasteur, Paris, France. Clone 13 and SARS-CoV were propagated in Vero cells. Viruses were handled exclusively in a biosafety level 3 facility. Recombinant human IFN- $\alpha$  B/D was purchased from PBL Biomedical Laboratories. Expression constructs for human IRF-7 were generated by amplifying cDNA from the plasmid pBS-hIRF7A (a kind gift from Luwen Zhang, Nebraska Center for Virology, UNL Biological Sciences, Lincoln, NE, USA) by PCR using the upstream primer 5'-CCGGATCGATATGGCTTGGCTCCTGAGAGGGCAGCCCCA-3' and the downstream primer 5'-CGCGCTCGAGCTAGGCGGGCTGCTCCAGCTCCATAAG-3', containing *Clal* and *XhoI* sites, respectively. The PCR product was introduced into the expression vector pCAGGs (Niwa *et al.*, 1991) by digestion with *Clal* and *XhoI* restriction endonucleases to obtain the construct pCAGGs-hIRF7A. The green fluorescent protein (GFP) fusion construct pCAGGs-GFP-hIRF7A was generated by introducing the hIRF7A open reading frame (ORF) via PCR into the expression plasmid pCAGGs-GFP. pCAGGs-GFP was generated by cloning the GFP ORF from pEGFP-C1 (Clontech) into the pCAGGs vector.

**RT-PCR analysis.** Total RNA was extracted from cells by using TriFast reagent (Qiagen) and treated with DNase I (Fermentas). For reverse transcription (RT), 1  $\mu$ g total RNA was incubated with 200 U SuperScript II reverse transcriptase (Gibco-BRL) and 100 ng random hexanucleotides in 20  $\mu$ l 1  $\times$  RT buffer (Gibco-BRL) supplied with 1 mM each dNTP, 20 U RNasin and 10 mM dithiothreitol. The resulting cDNA was amplified by 35 cycles of PCR, with each cycle consisting of 30 s at 94  $^{\circ}$ C, 1 min at 58  $^{\circ}$ C and 1 min at 72  $^{\circ}$ C, followed by 10 min at 72  $^{\circ}$ C. Primer sequences are available in Supplementary Table S1 (in JGV Online).

**GeneChip analysis.** The Affymetrix U133 Plus 2.0 array, which has complete coverage of the Human Genome U133 Set plus 6500 additional genes for analysis of over 47 000 transcripts, was used. GeneChip analysis was done according to the standard protocol provided by the manufacturer. Briefly, RNA was extracted by using TRIzol (Invitrogen) followed by purification using a Qiagen RNeasy Total RNA Isolation kit. Total RNA (10  $\mu$ g) was first reverse-transcribed by using a T7-oligo(dT) promoter primer in the first-strand cDNA synthesis reaction. Following RNase H-mediated second-strand cDNA synthesis, the double-stranded cDNA was purified and served as template in the subsequent *in vitro* transcription reaction, which was carried out in the presence of T7 RNA polymerase and a biotinylated nucleotide analogue/ribonucleotide mix for cRNA amplification and biotin labelling. The biotinylated cRNA targets were then cleaned up, fragmented and hybridized to GeneChip expression arrays. After washing and staining with streptavidin-phycoerythrin, signal intensity was scanned by using a GeneChip Scanner 3000. Results are reported in tabular format in Supplementary Table S2 (available in JGV Online).

**Real-time RT-PCR.** Total cellular RNA was isolated with a NucleoSpin RNA II kit (Macherey-Nagel) and eluted in 30  $\mu$ l double-distilled H<sub>2</sub>O. An aliquot of 600 ng RNA was then used as a template for cDNA synthesis, which was performed by using a QuantiTect RT kit (Qiagen) according to the manufacturer's instructions. mRNA levels of human  $\gamma$ -actin and IFN- $\beta$  were detected with QuantiTect primers QT00996415 and QT00203763, using a QuantiTect SYBR Green RT-PCR kit (Qiagen) and a LightCycler II (Roche).

**IFN assays.** Antiviral type I IFN in cell-culture supernatants was detected by using a highly sensitive bioassay (T. Kuri, M. Habjan, N. Penski & F. Weber, unpublished data). Briefly, supernatants of cells were harvested and SARS-CoV was inactivated by treatment with 0.05%  $\beta$ -propiolactone (Acros Organics) at 4  $^{\circ}$ C for 16 h.  $\beta$ -Propiolactone was hydrolysed by incubation at 37  $^{\circ}$ C for 2 h. Then, A549 cells seeded in 96-well dishes were incubated with the supernatants for 7 h and afterwards infected with a recombinant, IFN-sensitive Rift Valley fever virus (Habjan *et al.*, 2008) expressing *Renilla* luciferase. At 16 h post-infection, A549 cells were lysed with Passive Lysis buffer (Promega) and luciferase activity in lysates was determined by using the Dual Luciferase reporter assay (Promega). The amount of IFN present in the supernatants of infected cells was calculated by using dilutions of recombinant human IFN- $\alpha$  as standard.

**Western blot analysis.** Proteins were separated by SDS-PAGE and transferred to a PVDF membrane (Amersham), followed by incubation in PBS containing 5% non-fat dried milk and 0.05% Tween. The membrane was first incubated for 1 h with primary antibodies, and then washed three times with 0.05% PBS-Tween followed by incubation with a horseradish peroxidase (HRP)-conjugated secondary antibody. After three additional washing steps, detection was performed by using a SuperSignal West Femto chemiluminescence kit (Pierce). Primary antibody concentrations

used were 1:1000 for mouse anti-RIG-I, mouse anti-STAT-1 (Cell Signaling Technology) and mouse anti- $\beta$ -tubulin (Sigma).

**IRF-3 dimerization assays.** IRF-3 dimerization assays were carried out as described by Iwamura *et al.* (2001). Briefly, infected cells were lysed in protein lysis buffer [50 mM Tris/HCl (pH 7.5), 150 mM NaCl, 1 mM EDTA, 1% Nonidet P-40] containing protease inhibitors (Complete Protease Inhibitor; Roche) and phosphatase inhibitors (Phosphatase Inhibitor Cocktail II; Calbiochem), vortexed, incubated on ice for 10 min and then centrifuged at 4 °C for 5 min at 10 000 g. Cell extracts (10  $\mu$ g protein) were then analysed by non-denaturing gel electrophoresis in a 10% native gel. Cathode buffer contained 1% deoxycholate. IRF-3 monomers and dimers were detected after blotting onto an Immobilon-P membrane (Millipore), using a 1:500 dilution of the rabbit polyclonal anti-IRF-3 antibody FL-425 (Santa Cruz).

**IRF nuclear-translocation assay.** Endogenous IRF-3 was detected in Vero cells by enzymic amplification of the immunofluorescence signal. Cells were grown on coverslips, treated with IFN and infected with SARS-CoV as indicated. After an incubation period of 16 h, cells were fixed with 3% paraformaldehyde and permeabilized with 0.5% Triton X-100 dissolved in PBS. Cells were washed three times with PBS and incubated with the primary antibodies polyclonal rabbit anti-SARS-CoV N protein and monoclonal mouse anti-IRF-3 17C2 (Spiegel *et al.*, 2005), diluted 1:1000 and 1:500, respectively, in TNB blocking buffer (Perkin Elmer). After incubation at room temperature for 1 h, the coverslips were washed three times in PBS, then treated with the secondary antibodies, Cy3-conjugated goat anti-rabbit IgG (Alexis) and biotin-conjugated anti-mouse (Perkin Elmer) at a dilution of 1:200 each. Cells were again washed three times in PBS and incubated for 30 min with streptavidin-conjugated HRP (Perkin Elmer) at a dilution of 1:100. After washing in PBS, cells were incubated for 5 min in Fluorophore Tyramide amplification reagent (Perkin Elmer), then washed in PBS and mounted by using Fluorsave solution (Calbiochem).

For detection of IRF-7, Vero cells were transfected with 500 ng pCAGGS-GFP-hIRF7A and 1  $\mu$ g pCAGGS-hIRF7A in 200  $\mu$ l OptiMEM (Invitrogen) containing 4.5  $\mu$ l FugeneHD (Roche). At 48 h post-transfection, cells were infected for 8 h with SARS-CoV at an m.o.i. of 1, fixed with 3% paraformaldehyde and permeabilized with 0.5% Triton X-100 dissolved in PBS. For immunofluorescence analysis, cells were washed three times with PBS and then incubated with the mouse monoclonal anti-SARS-CoV N (Spiegel *et al.*, 2005) diluted 1:500 in PBS. To counterstain the nuclear DNA, 4',6-diamidino-2-phenylindole (DAPI, stock solution of 5  $\mu$ g ml<sup>-1</sup>) was added at a dilution of 1:500.

Stained cell samples were examined by using a Zeiss Axioplan 2 imaging microscope with a  $\times 63$  NA1.4 objective.

## RESULTS

### IFN priming triggers a transcriptional IFN response to SARS-CoV

We investigated whether cells could become responsive to SARS-CoV if they were primed with IFN. As an experimental system, we used human 293lp cells, which are fully IFN-competent and support productive virus infection (Spiegel & Weber, 2006). These cells were first treated with different amounts of human IFN- $\alpha$  and then infected with SARS-CoV at an m.o.i. of 1. After an incubation period of 16 h, total RNA was extracted and

cellular gene expression was analysed by RT-PCR. Fig. 1 (panel 1) shows that, as expected, no IFN- $\beta$  transcription is induced by SARS-CoV in unprimed cells. Similarly, in uninfected cells, IFN- $\beta$  transcription is not induced by IFN- $\alpha$ , as the main transcription factor IRF-3 is not activated by IFN (Honda & Taniguchi, 2006). However, in cells that were both pretreated with 100 U IFN ml<sup>-1</sup> and subsequently infected with SARS-CoV, a clear signal for IFN- $\beta$  mRNA was detectable, suggesting IFN gene upregulation. Control RT-PCRs for the viral N mRNA and the  $\gamma$ -actin housekeeping gene demonstrate that similar amounts of input RNA had been used and that priming with 100 U IFN- $\alpha$  ml<sup>-1</sup> did not affect virus replication significantly (Fig. 1, panels 2 and 3). This latter observation is in line with a study showing that up to 500 U IFN ml<sup>-1</sup> has no effect on SARS-CoV titres (Stroher *et al.*, 2004).

These data suggest that the inability of cells to transcribe the IFN- $\beta$  gene in response to SARS-CoV can be overcome by a preceding upregulation of IFN-stimulated genes (ISGs).

### Gene-expression profiles of IFN-primed and SARS-CoV-infected cells

IFN priming may change the cellular response to SARS-CoV infection. To investigate this in more depth, we performed RT-PCR analysis of a series of selected genes involved in innate immunity. As shown in Fig. 2, transcription of the genes for DDX58 (RIG-I) as well as for IFIH1 (MDA5), IRF-7, STAT-1, IFIT1, IFIT2, IFIT3, MxA, OAS1, CXCL10 (IP-10) and CXCL11 is upregulated synergistically by IFN and SARS-CoV, whereas IFN treatment or SARS-CoV infection alone did not result in such a strong response. These findings suggest that priming with small amounts of IFN enables cells to launch a typical IFN response to SARS-CoV infection. To evaluate this

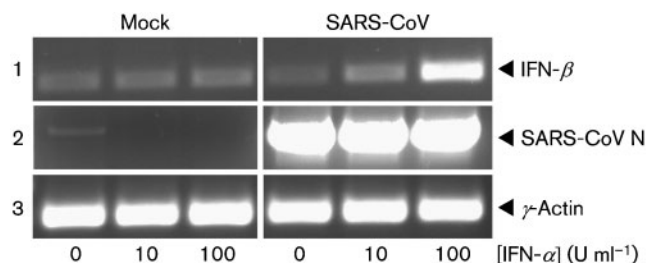


**Fig. 1.** Priming with IFN- $\alpha$  licenses cells to induce IFN- $\beta$  gene transcription in response to SARS-CoV. RT-PCR analysis: human 293lp cells were treated with 0, 10 or 100 U recombinant human IFN- $\alpha$  B/D ml<sup>-1</sup>, incubated for 24 h and then infected with SARS-CoV at an m.o.i. of 1. At 16 h post-infection, total RNA was isolated from cells and assayed for the presence of mRNA for IFN- $\beta$  (panel 1), the N gene of SARS-CoV (panel 2) and the cellular  $\gamma$ -actin gene (panel 3).

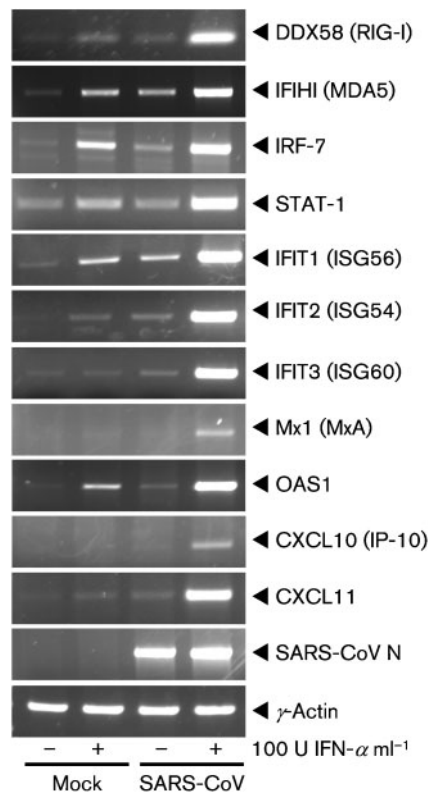


**Fig. 2.** Genes influenced by IFN and SARS-CoV. 293lp cells were treated with either 0 or 100 U human IFN- $\alpha$  ml $^{-1}$ , incubated for 24 h and then infected with SARS-CoV or mock-infected. At 16 h post-infection, total RNA was isolated and assayed by RT-PCR for the indicated genes.

assumption in a more global manner, we employed microarray analysis of uninfected 293lp cells versus cells that were both IFN-primed and infected, using Affymetrix Human Genome U133 Plus 2.0 GeneChip arrays. Cellular mRNA was amplified from total RNA and tested for quality and integrity by gel electrophoresis. After cDNA synthesis, biotinylated cRNAs were produced by *in vitro* transcription and hybridized to cDNA arrays representing 47 000 transcripts and variants. Hybridization was monitored by incubation with streptavidin-conjugated phycoerythrin and the fluorescence signal was scanned automatically. Supplementary Table S2 (available in JGV Online) shows that the genes upregulated most strongly by the combination of IFN and SARS-CoV were indeed components of the IFN-induction and -response signalling pathways, such as DDX58 (RIG-I), IFIHI (MDA5), IRF-7 and STAT-1, several IFN effector molecules such as IFIT1, IFIT2, IFIT3, MxA, OAS1 and TRIM22, the ubiquitin-like molecule ISG15 and the cytokines/chemokines CXCL10, CXCL11 and IFN- $\beta$ . Thus, in agreement with the RT-PCR results (see Fig. 2), the global gene-expression analysis demonstrates that the response to SARS-CoV is biased strongly towards an IFN response if cells are pretreated with IFN.

### Translational response of IFN-primed and SARS-CoV-infected cells

To follow up on our observations, we sought to measure IFN concentrations in cell supernatants. Initially, we used a commercial ELISA kit, but were unable to detect any secreted IFN- $\beta$  after priming and infection with SARS-CoV (data not shown). As this finding raised the possibility that the IFN induction levels may be too low for this kind of assay, we decided to reassess both IFN transcription and production by more sensitive and quantitative methods. We (i) employed a real-time RT-PCR protocol for IFN- $\beta$  mRNA and (ii) established a sensitive bioassay to measure antivirally active IFNs. A strong IFN inducer, the Rift Valley fever virus mutant Clone 13 (Billecocq *et al.*, 2004), was used as standard and additional control. The dose-response curve in Fig. 3(a) shows that increasing amounts of the IFN-inducing control virus result in increasing levels of IFN- $\beta$  mRNA, and that even a 10-fold upregulation of IFN transcription can be detected by real-time RT-PCR. Moreover, results from the priming experiment confirm that IFN treatment alone and SARS-CoV infection alone did not result in a substantial IFN induction, whereas the combination of both induced IFN- $\beta$  mRNA by over 1000-fold. Measurement of the corresponding IFN levels in the supernatants (Fig. 3b) shows that the transcriptional induction by SARS-CoV in IFN-primed cells results in production of approximately 3 U IFN (ml supernatant) $^{-1}$ . A comparison with the standard curve obtained with the control virus indicated that these low, but clearly measurable, levels are within the range expected after a 1000-fold upregulation of IFN- $\beta$  mRNA [please note that the  $y$ -axis of Fig. 3(a) is displayed as a log $_{10}$  scale and that of Fig. 3(b) as a linear scale].

We wondered whether the transcriptional response to SARS-CoV in cells that were primed with IFN would be sufficient for detectable protein production besides IFN. We chose two ISGs that are prominently transcribed and are important for the IFN response, namely RIG-I, an important RNA sensor of IFN induction (Yoneyama & Fujita, 2007), and STAT-1, the master regulator of IFN signalling (Levy & Darnell, 2002). These genes are clearly upregulated by the combination of IFN priming and SARS-CoV infection (see Fig. 2). In line with this, Western blot analysis of protein levels shows that concentrations of both RIG-I and STAT-1 proteins increase clearly and strongly in SARS-CoV-infected cells primed with IFN (Fig. 4).

Thus, taken together, our results suggest that IFN priming allows cells to bypass the IFN-inhibitory mechanisms of SARS-CoV to some extent, resulting in a typical IFN response.

### Activation status of IRF-3 and IRF-7

We have shown previously that, in cells infected with SARS-CoV, the IFN- $\beta$  transcription factor IRF-3 neither dimerizes nor accumulates stably in the nucleus, indicating

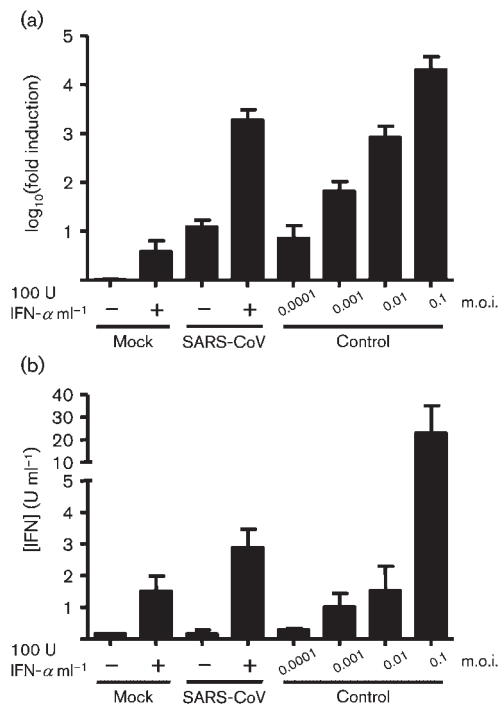


**Fig. 3.** IFN synthesis by primed cells. Human 293p cells were IFN-treated and virus-infected as described for Fig. 2. In parallel, cells were infected with increasing amounts of an IFN-inducing control virus. Supernatants were collected and cells were lysed to isolate total RNA. Transcriptional induction of the IFN-β gene (a) and IFN concentrations in the supernatants (b) were determined by real-time RT-PCR and a bioassay, respectively. Experiments were repeated three times; mean +SD values are shown. The spurious amounts of IFN detected in the supernatant of primed mock-infected cells probably represent residual priming IFN.

a lack of activation (Spiegel *et al.*, 2005). We wondered whether IFN priming may allow cells to return to a full IRF-3 response. To investigate dimerization of IRF-3, we used non-denaturing gel electrophoresis coupled to

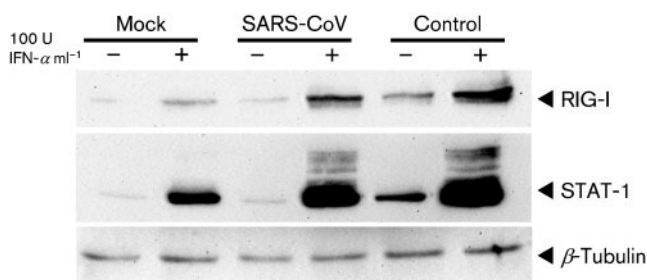


**Fig. 4.** Endogenous protein synthesis by primed cells. Human 293p cells were IFN-treated and virus-infected as described for Fig. 2. The control virus was used at an m.o.i. of 1. Cells were lysed in RIPA buffer and whole-cell protein was assayed by immunoblot analysis for the presence of RIG-I, STAT-1 and β-tubulin.

Western blot analysis (Iwamura *et al.*, 2001). Fig. 5(a) shows that, much to our surprise, in IFN-primed cells, IRF-3 is still present as a monomer after SARS-CoV infection. The control virus triggered IRF-3 dimerization as expected. Moreover, IFN priming also did not allow nuclear import of IRF-3 in response to SARS-CoV (Fig. 5b), similar to what was observed in unprimed cells. From these data, we had to conclude that the impact of SARS-CoV on the visible activation state of IRF-3 cannot be alleviated by IFN pretreatment.

RT-PCR analyses have demonstrated that IRF-7 is among the genes upregulated by IFN priming (see Fig. 2 and Supplementary Table S2). IRF-7 is homologous to IRF-3 and is thought to substitute for it at later time points of the IFN response (Sato *et al.*, 2000). IRF-7 could thus be responsible for the SARS-CoV-induced IFN-β gene transcription after IFN priming. However, we were unable to detect endogenous IRF-7 by immunofluorescence analysis using various antibodies. Therefore, we expressed a GFP-IRF-7 fusion construct instead and superinfected cells afterwards with SARS-CoV. Fig. 6 (upper panel) shows that the control virus induces nuclear import of GFP-IRF-7, indicating the suitability of the assay. In cells infected with SARS-CoV, however, IRF-7 remained in the cytoplasm (Fig. 6, middle panel) in a similar manner to uninfected cells (data not shown). The same observations were

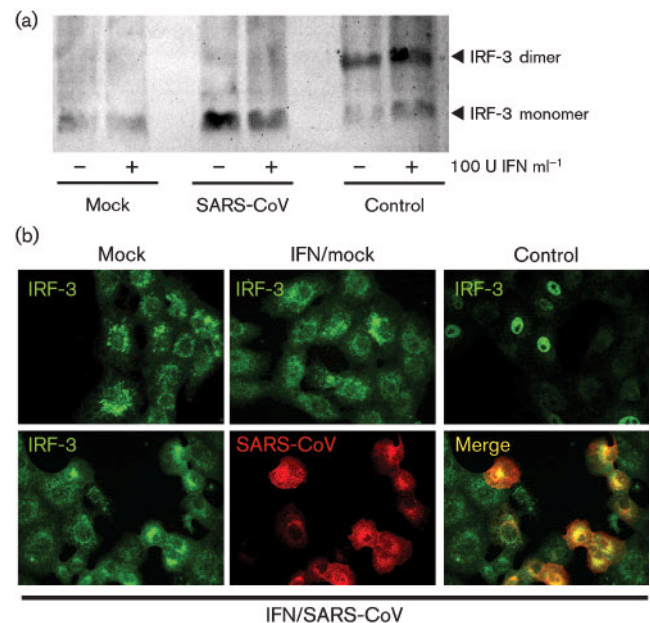


**Fig. 5.** Activation of IRF-3. (a) Homodimerization assay. Extracts from 293p cells primed with IFN and infected with SARS-CoV or the control virus as described for Fig. 4 were analysed by non-denaturing gel electrophoresis followed by an immunoblot to detect IRF-3. (b) Subcellular localization. IFN-primed and virus-infected Vero cells were analysed by indirect immunofluorescence using antibodies specific for IRF-3 and SARS-CoV.

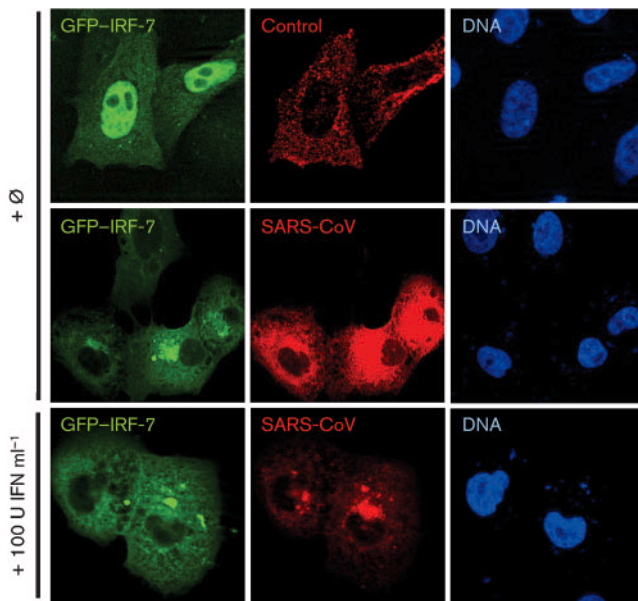


**Fig. 6.** Activation of IRF-7. Vero cells were transfected with a GFP-IRF-7 cDNA construct and IFN-treated and infected as indicated. Subcellular localization of IRF-7 was analysed by GFP autofluorescence, and virus infection by immunofluorescence using antibodies specific for SARS-CoV and the control virus, respectively.

obtained when cells had been primed with IFN prior to infection (Fig. 6, lower panel). Thus, visible activation of IRF-7 is not detectable in SARS-CoV-infected cells, in a manner similar to that observed for IRF-3. To our knowledge, this is the first report on the absence of detectable IRF-7 activation by SARS-CoV.

Taken together, despite the fact that IFN pretreatment licenses cells to transcribe IFN- $\beta$  as well as other IRF-driven genes and ISGs in response to SARS-CoV, we were unable to find evidence of IRF-3 or IRF-7 activation.

## DISCUSSION

Previous work from our laboratory and from other groups has established that IFN transcription is blocked in tissue cells infected with SARS-CoV (Cheung *et al.*, 2005; Frieman *et al.*, 2008; Spiegel *et al.*, 2005; Spiegel & Weber, 2006; Thiel & Weber, 2008). Our results presented here imply that priming with small amounts of IFN allows cells to partially restore their innate immune responsiveness to SARS-CoV.

Even for the weak IFN inducer SARS-CoV, IFN priming and virus sensing appear to act together in an unexpectedly tight and synergistic manner. This indicates that the positive-feedback loop caused by IFN priming is able to amplify the antiviral effect of physiological levels of IFN. Most likely, the heightened IFN induction by primed cells

is due to an upregulation of the virus-sensing signalling chain, exemplified by molecules such as MDA5 and IRF-7. This may result in a state of 'raised awareness' for the cell, as MDA5 is the intracellular sensor for coronaviruses (Roth-Cross *et al.*, 2008) and IRF-7 is a potent regulator of the IFN system (Honda *et al.*, 2005). Interestingly, TLR7, the endosomal sensor for coronavirus infection (Cervantes-Barragan *et al.*, 2007), was not among the upregulated genes (see Supplementary Table S2). By any means, the priming mechanism allows the host to relay the IFN signal and to couple maximal production of antiviral and proinflammatory cytokines to ongoing virus infection, thus restricting these potentially damaging cytokines to those sites where they are needed most. Moreover, previous exposure to IFN apparently allows cells to alleviate the action of viral IFN antagonists.

In contrast to tissue cells, pDCs transcribe and translate as much IFN in response to SARS-CoV as in response to the strong IFN inducer Newcastle disease virus (Cervantes-Barragan *et al.*, 2007). The pronounced response of pDCs had initially prompted us to ask whether, *in vivo*, the IFN produced by pDCs could prime neighbouring tissue cells, thus helping them to launch a full IFN response to SARS-CoV. Our results showing that this is at least partially the case indicate that, *in vivo*, the pDC-derived IFN may help neighbouring cells to overcome their anergic state of responsiveness to SARS-CoV, and to produce IFN themselves. As levels of IFN are rather low, however, the fine balance between IFN production and virus load may determine the net outcome of infection. In fact, most studies involving patient materials found no significant upregulation of type I IFNs or of IFN-induced genes (reviewed by Frieman *et al.*, 2008; Thiel & Weber, 2008). However, a recent study investigating immune responses of 40 clinically well-defined SARS cases revealed high levels of plasma IFN and an atypical ISG-expression profile in pre-crisis patients, but not in crisis patients (Cameron *et al.*, 2007). In agreement with this, it has been shown that SARS-CoV infection triggers an early type I IFN response in cynomolgus macaques (de Lang *et al.*, 2007). Possibly, pDC-derived IFN may appear early in infection, but at the time when patients are admitted to hospital, it has become undetectable due to dilution or exhaustion of pDCs and primed tissue cells. In SARS survivors, a strong initial IFN response started by pDCs and amplified by primed tissue cells may eventually control virus infection.

IFN treatment, which was shown to protect experimentally infected macaques from SARS-CoV infection (Haagmans *et al.*, 2004), may thus have a double benefit in that it allows cells to at least partially restore their antiviral responsiveness.

SARS-CoV is capable of blocking IFN induction at several levels. Firstly, the viral dsRNA produced during infection (Weber *et al.*, 2006) is stored away in distinct membrane compartments in order to minimize host-cell recognition (Knoops *et al.*, 2008; Versteeg *et al.*, 2007). Secondly, there is a range of active measures. In overexpression studies, it

was shown that the viral proteins ORF3b, ORF6 and N (Kopecky-Bromberg *et al.*, 2007) are able to inhibit IRF-3 directly, and that the PLpro domain, part of the viral nsp3 protein, inhibits activation of IRF-3-dependent promoters (Devaraj *et al.*, 2007). Moreover, the nsp1 protein induces a general RNA instability that can affect IFN- $\beta$  mRNA levels (Kamitani *et al.*, 2006). Therefore, viruses with mutations in the nsp1 gene induce higher IFN levels than wild-type virus (Narayanan *et al.*, 2008; Wathelet *et al.*, 2007). In line with these results, our study indicates that IRF-7, the master regulator of the IFN system (Honda *et al.*, 2005), is not activated by SARS-CoV. It will be interesting to see whether a specific viral gene product is responsible for this.

In spite of all these well-described inhibitory mechanisms, IFN pretreatment allows cells to at least partially bypass them. Interestingly, a similar observation was obtained with DCs infected with influenza viruses (Osterlund *et al.*, 2005; Phipps-Yonas *et al.*, 2008). Comparison of SARS-CoV with the highly effective IFN inducer Clone 13, however (see Fig. 4), reveals that the response is not yet at its upper limit, indicating that viral countermeasures and hiding mechanisms are still in place to some extent. Interestingly, previous studies have shown that, in SARS-CoV-infected cells that were superinfected with Sendai virus, IFN- $\beta$  mRNA was transcribed to the same level as in cells infected with Sendai virus only (Versteeg *et al.*, 2007). For SARS-CoV (and the related mouse hepatitis virus), it was additionally shown that secretion of IFN- $\beta$  is inhibited in such double-infected cells, despite a clear transcriptional induction (Devaraj *et al.*, 2007; Roth-Cross *et al.*, 2007). In our study, however, we detected amounts of secreted IFN in a range expected from the level of transcriptional induction. Differences in experimental set-up may account for the conflicting observations. Coronavirus infection was fully established in those cells superinfected with Sendai virus, whereas in the case of our priming studies, SARS-CoV first had to pass through all phases of the multiplication cycle and accumulate its gene products. It may thus be that, in a fully established coronavirus infection, which is known to reorganize large parts of the internal cell membranes (Knoops *et al.*, 2008; Stertz *et al.*, 2007), secretion of cytokines does not take place any more, whereas in earlier infection phases, this is not the case. Alternatively, IFN priming may be able to neutralize the secretion block imposed by SARS-CoV.

An unexpected finding of our study was that, despite a clear upregulation of IFN- $\beta$  transcription, neither IRF-3 nor IRF-7 was visibly activated. At least for IRF-3, however, several reports indicate that transactivation of promoters can occur without any of the conventional signs of activation (Collins *et al.*, 2004; Noyce *et al.*, 2009). This confirms the view that IRF-3 is activated in a multi-phase manner and that subdetectable amounts of IRF-3 are sufficient for a certain promoter activity (Clement *et al.*, 2008). Quantification of IFN transcription in dependence of inducer RNA concentrations or infection phase,

correlated with assays measuring dimer formation and nuclear import, may allow better definition of the different phases of IRF-3 activity.

To sum up, we have shown that the large array of anti-IFN strategies employed by SARS-CoV is partly mitigated in cells that have been in contact with IFN before infection. Moreover, IFN-primed cells infected with SARS-CoV display a lack of correlation between IFN- $\beta$  transcription and the conventional assays used to measure the activity of IRF-3 and IRF-7.

## ACKNOWLEDGEMENTS

We thank Valentina Wagner for excellent technical assistance and Otto Haller for constant support and advice. We are indebted to Estanis Nistal-Villán (Mount Sinai School of Medicine), Stephan Becker, Michèle Bouloy and Luwen Zhang for providing essential reagents. Work in our laboratories is supported by grant 01 KI 0705 of the Bundesministerium für Bildung und Forschung (F.W.), grant U19AI62623 from NIAID (A.G.-S.) and the start-up fund KSF0062 of the Shanghai Public Health Clinical Centre (X.Z.).

## REFERENCES

- Billecocq, A., Spiegel, M., Vialat, P., Kohl, A., Weber, F., Bouloy, M. & Haller, O. (2004). NSs protein of Rift Valley fever virus blocks interferon production by inhibiting host gene transcription. *J Virol* **78**, 9798–9806.
- Caillaud, A., Hovanessian, A. G., Levy, D. E. & Marie, I. J. (2005). Regulatory serine residues mediate phosphorylation-dependent and phosphorylation-independent activation of interferon regulatory factor 7. *J Biol Chem* **280**, 17671–17677.
- Cameron, M. J., Ran, L., Xu, L., Danesh, A., Bermejo-Martin, J. F., Cameron, C. M., Muller, M. P., Gold, W. L., Richardson, S. E. & other authors (2007). Interferon-mediated immunopathological events are associated with atypical innate and adaptive immune responses in severe acute respiratory syndrome (SARS) patients. *J Virol* **81**, 8692–8706.
- Cervantes-Barragan, L., Zust, R., Weber, F., Spiegel, M., Lang, K. S., Akira, S., Thiel, V. & Ludewig, B. (2007). Control of coronavirus infection through plasmacytoid dendritic-cell-derived type I interferon. *Blood* **109**, 1131–1137.
- Cheung, C. Y., Poon, L. L., Ng, I. H., Luk, W., Sia, S. F., Wu, M. H., Chan, K. H., Yuen, K. Y., Gordon, S. & other authors (2005). Cytokine responses in severe acute respiratory syndrome coronavirus-infected macrophages *in vitro*: possible relevance to pathogenesis. *J Virol* **79**, 7819–7826.
- Cinatl, J., Morgenstern, B., Bauer, G., Chandra, P., Rabenau, H. & Doerr, H. W. (2003). Treatment of SARS with human interferons. *Lancet* **362**, 293–294.
- Clement, J. F., Bibeau-Poirier, A., Gravel, S. P., Grandvaux, N., Bonneil, E., Thibault, P., Meloche, S. & Servant, M. J. (2008). Phosphorylation of IRF-3 on Ser 339 generates a hyperactive form of IRF-3 through regulation of dimerization and CBP association. *J Virol* **82**, 3984–3996.
- Collins, S. E., Noyce, R. S. & Mossman, K. L. (2004). Innate cellular response to virus particle entry requires IRF3 but not virus replication. *J Virol* **78**, 1706–1717.
- de Lang, A., Baas, T., Teal, T., Leijten, L. M., Rain, B., Osterhaus, A. D., Haagmans, B. L. & Katze, M. G. (2007). Functional genomics

- highlights differential induction of antiviral pathways in the lungs of SARS-CoV infected macaques. *PLoS Pathog* 3, e112.
- Denison, M. R. (2004).** Severe acute respiratory syndrome coronavirus pathogenesis, disease and vaccines: an update. *Pediatr Infect Dis J* 23, S207–S214.
- Devaraj, S. G., Wang, N., Chen, Z., Chen, Z., Tseng, M., Barretto, N., Lin, R., Peters, C. J., Tseng, C. T. & other authors (2007).** Regulation of IRF-3-dependent innate immunity by the papain-like protease domain of the severe acute respiratory syndrome coronavirus. *J Biol Chem* 282, 32208–32221.
- Drosten, C., Gunther, S., Preiser, W., van der Werf, S., Brodt, H. R., Becker, S., Rabenau, H., Panning, M., Kolesnikova, L. & other authors (2003).** Identification of a novel coronavirus in patients with severe acute respiratory syndrome. *N Engl J Med* 348, 1967–1976.
- Erlandsson, L., Blumenthal, R., Eloranta, M. L., Engel, H., Alm, G., Weiss, S. & Leanderson, T. (1998).** Interferon- $\beta$  is required for interferon- $\alpha$  production in mouse fibroblasts. *Curr Biol* 8, 223–226.
- Frieman, M., Heise, M. & Baric, R. (2008).** SARS coronavirus and innate immunity. *Virus Res* 133, 101–112.
- Graham, F. L., Smiley, J., Russell, W. C. & Nairn, R. (1977).** Characteristics of a human cell line transformed by DNA from human adenovirus type 5. *J Gen Virol* 36, 59–74.
- Gu, J., Gong, E., Zhang, B., Zheng, J., Gao, Z., Zhong, Y., Zou, W., Zhan, J., Wang, S. & other authors (2005).** Multiple organ infection and the pathogenesis of SARS. *J Exp Med* 202, 415–424.
- Haagmans, B. L., Kuiken, T., Martina, B. E., Fouchier, R. A., Rimmelzwaan, G. F., Van Amerongen, G., Van Riel, D., De Jong, T., Itamura, S. & other authors (2004).** Pegylated interferon- $\alpha$  protects type 1 pneumocytes against SARS coronavirus infection in macaques. *Nat Med* 10, 290–293.
- Habjan, M., Penski, N., Spiegel, M. & Weber, F. (2008).** T7 RNA polymerase-dependent and -independent systems for cDNA-based rescue of Rift Valley fever virus. *J Gen Virol* 89, 2157–2166.
- Hiscott, J. (2007).** Triggering the innate antiviral response through IRF-3 activation. *J Biol Chem* 282, 15325–15329.
- Honda, K. & Taniguchi, T. (2006).** IRFs: master regulators of signalling by Toll-like receptors and cytosolic pattern-recognition receptors. *Nat Rev Immunol* 6, 644–658.
- Honda, K., Yanai, H., Negishi, H., Asagiri, M., Sato, M., Mizutani, T., Shimada, N., Ohba, Y., Takaoka, A. & other authors (2005).** IRF-7 is the master regulator of type-I interferon-dependent immune responses. *Nature* 434, 772–777.
- Iwamura, T., Yoneyama, M., Yamaguchi, K., Suhara, W., Mori, W., Shiota, K., Okabe, Y., Namiki, H. & Fujita, T. (2001).** Induction of IRF-3/-7 kinase and NF- $\kappa$ B in response to double-stranded RNA and virus infection: common and unique pathways. *Genes Cells* 6, 375–388.
- Kamitani, W., Narayanan, K., Huang, C., Lokugamage, K., Ikegami, T., Ito, N., Kubo, H. & Makino, S. (2006).** Severe acute respiratory syndrome coronavirus nsp1 protein suppresses host gene expression by promoting host mRNA degradation. *Proc Natl Acad Sci U S A* 103, 12885–12890.
- Knoops, K., Kikkert, M., Worm, S. H., Zevenhoven-Dobbe, J. C., van der Meer, Y., Koster, A. J., Mommaas, A. M. & Snijder, E. J. (2008).** SARS-coronavirus replication is supported by a reticulovesicular network of modified endoplasmic reticulum. *PLoS Biol* 6, e226.
- Kopecky-Bromberg, S. A., Martinez-Sobrido, L., Frieman, M., Baric, R. A. & Palese, P. (2007).** Severe acute respiratory syndrome coronavirus open reading frame (ORF) 3b, ORF 6, and nucleocapsid proteins function as interferon antagonists. *J Virol* 81, 548–557.
- Ksiazek, T. G., Erdman, D., Goldsmith, C. S., Zaki, S. R., Peret, T., Emery, S., Tong, S., Urbani, C., Comer, J. A. & other authors (2003).** A novel coronavirus associated with severe acute respiratory syndrome. *N Engl J Med* 348, 1953–1966.
- Kuiken, T., Fouchier, R. A., Schutten, M., Rimmelzwaan, G. F., van Amerongen, G., van Riel, D., Laman, J. D., de Jong, T., van Doornum, G. & other authors (2003).** Newly discovered coronavirus as the primary cause of severe acute respiratory syndrome. *Lancet* 362, 263–270.
- Levy, D. E. & Darnell, J. E., Jr (2002).** Stats: transcriptional control and biological impact. *Nat Rev Mol Cell Biol* 3, 651–662.
- Marie, I., Durbin, J. E. & Levy, D. E. (1998).** Differential viral induction of distinct interferon- $\alpha$  genes by positive feedback through interferon regulatory factor-7. *EMBO J* 17, 6660–6669.
- Narayanan, K., Huang, C., Lokugamage, K., Kamitani, W., Ikegami, T., Tseng, C. T. & Makino, S. (2008).** Severe acute respiratory syndrome coronavirus nsp1 suppresses host gene expression, including that of type I interferon, in infected cells. *J Virol* 82, 4471–4479.
- Niwa, H., Yamamura, K. & Miyazaki, J. (1991).** Efficient selection for high-expression transfectants with a novel eukaryotic vector. *Gene* 108, 193–199.
- Noyce, R. S., Collins, S. E. & Mossman, K. L. (2009).** Differential modification of interferon regulatory factor 3 following virus particle entry. *J Virol* 83, 4013–4022.
- Osterlund, P., Veckman, V., Siren, J., Klucher, K. M., Hiscott, J., Matikainen, S. & Julkunen, I. (2005).** Gene expression and antiviral activity of alpha/beta interferons and interleukin-29 in virus-infected human myeloid dendritic cells. *J Virol* 79, 9608–9617.
- Peiris, J. S., Chu, C. M., Cheng, V. C., Chan, K. S., Hung, I. F., Poon, L. L., Law, K. I., Tang, B. S., Hon, T. Y. & other authors (2003a).** Clinical progression and viral load in a community outbreak of coronavirus-associated SARS pneumonia: a prospective study. *Lancet* 361, 1767–1772.
- Peiris, J. S., Lai, S. T., Poon, L. L., Guan, Y., Yam, L. Y., Lim, W., Nicholls, J., Yee, W. K., Yan, W. W. & other authors (2003b).** Coronavirus as a possible cause of severe acute respiratory syndrome. *Lancet* 361, 1319–1325.
- Peiris, J. S., Guan, Y. & Yuen, K. Y. (2004).** Severe acute respiratory syndrome. *Nat Med* 10, S88–S97.
- Phipps-Yonas, H., Seto, J., Sealfon, S. C., Moran, T. M. & Fernandez-Sesma, A. (2008).** Interferon- $\beta$  pretreatment of conventional and plasmacytoid human dendritic cells enhances their activation by influenza virus. *PLoS Pathog* 4, e1000193.
- Pichlmair, A. & Reis e Sousa, C. (2007).** Innate recognition of viruses. *Immunity* 27, 370–383.
- Roth-Cross, J. K., Martinez-Sobrido, L., Scott, E. P., Garcia-Sastre, A. & Weiss, S. R. (2007).** Inhibition of the alpha/beta interferon response by mouse hepatitis virus at multiple levels. *J Virol* 81, 7189–7199.
- Roth-Cross, J. K., Bender, S. J. & Weiss, S. R. (2008).** Murine coronavirus mouse hepatitis virus is recognized by MDA5 and induces type I interferon in brain macrophages/microglia. *J Virol* 82, 9829–9838.
- Sadler, A. J. & Williams, B. R. (2008).** Interferon-inducible antiviral effectors. *Nat Rev Immunol* 8, 559–568.
- Samuel, C. E. (2001).** Antiviral actions of interferons. *Clin Microbiol Rev* 14, 778–809.
- Sato, M., Suemori, H., Hata, N., Asagiri, M., Ogasawara, K., Nakao, K., Nakaya, T., Katsuki, M., Noguchi, S. & other authors (2000).** Distinct and essential roles of transcription factors IRF-3 and IRF-7 in response to viruses for IFN- $\alpha$ /beta gene induction. *Immunity* 13, 539–548.
- Spiegel, M. & Weber, F. (2006).** Inhibition of cytokine gene expression and induction of chemokine genes in non-lymphatic cells infected with SARS coronavirus. *Virol J* 3, 17.

- Spiegel, M., Pichlmair, A., Martinez-Sobrido, L., Cros, J., Garcia-Sastre, A., Haller, O. & Weber, F. (2005).** Inhibition of beta interferon induction by severe acute respiratory syndrome coronavirus suggests a two-step model for activation of interferon regulatory factor 3. *J Virol* **79**, 2079–2086.
- Stertz, S., Reichelt, M., Spiegel, M., Kuri, T., Martinez-Sobrido, L., Garcia-Sastre, A., Weber, F. & Kochs, G. (2007).** The intracellular sites of early replication and budding of SARS-coronavirus. *Virology* **361**, 304–315.
- Stewart, W. E., II, Gosser, L. B. & Lockart, R. Z., Jr (1971).** Priming: a nonantiviral function of interferon. *J Virol* **7**, 792–801.
- Stroher, U., DiCaro, A., Li, Y., Strong, J. E., Aoki, F., Plummer, F., Jones, S. M. & Feldmann, H. (2004).** Severe acute respiratory syndrome-related coronavirus is inhibited by interferon- $\alpha$ . *J Infect Dis* **189**, 1164–1167.
- Suhara, W., Yoneyama, M., Kitabayashi, I. & Fujita, T. (2002).** Direct involvement of CREB-binding protein/p300 in sequence-specific DNA binding of virus-activated interferon regulatory factor-3 holocomplex. *J Biol Chem* **277**, 22304–22313.
- Thiel, V. & Weber, F. (2008).** Interferon and cytokine responses to SARS-coronavirus infection. *Cytokine Growth Factor Rev* **19**, 121–132.
- Versteeg, G. A., Bredenbeek, P. J., van den Worm, S. H. & Spaan, W. J. (2007).** Group 2 coronaviruses prevent immediate early interferon induction by protection of viral RNA from host cell recognition. *Virology* **361**, 18–26.
- Wathelet, M. G., Orr, M., Frieman, M. B. & Baric, R. S. (2007).** Severe acute respiratory syndrome coronavirus evades antiviral signaling: role of nsp1 and rational design of an attenuated strain. *J Virol* **81**, 11620–11633.
- Weaver, B. K., Kumar, K. P. & Reich, N. C. (1998).** Interferon regulatory factor 3 and CREB-binding protein/p300 are subunits of double-stranded RNA-activated transcription factor DRAF1. *Mol Cell Biol* **18**, 1359–1368.
- Weber, F., Wagner, V., Rasmussen, S. B., Hartmann, R. & Paludan, S. R. (2006).** Double-stranded RNA is produced by positive-strand RNA viruses and DNA viruses but not in detectable amounts by negative-strand RNA viruses. *J Virol* **80**, 5059–5064.
- WHO (2004).** Summary of probable SARS cases with onset of illness from 1 November 2002 to 31 July 2003. [http://www.who.int/csr/sars/country/table2004\\_04\\_21/en/index.html](http://www.who.int/csr/sars/country/table2004_04_21/en/index.html)
- Yoneyama, M. & Fujita, T. (2007).** Function of RIG-I-like receptors in antiviral innate immunity. *J Biol Chem* **282**, 15315–15318.
- Yoneyama, M. & Fujita, T. (2008).** Structural mechanism of RNA recognition by the RIG-I-like receptors. *Immunity* **29**, 178–181.